

ScanQA: 3D Question Answering for Spatial Scene Understanding

Daichi Azuma*
Kyoto University

Taiki Miyanishi*
ATR, RIKEN AIP

Shuhe Kurita*
RIKEN, JST PRESTO

Motoki Kawanabe
ATR, RIKEN AIP

Abstract

We propose a new 3D spatial understanding task of 3D Question Answering (3D-QA). In the 3D-QA task, models receive visual information from the entire 3D scene of the rich RGB-D indoor scan and answer the given textual questions about the 3D scene. Unlike the 2D-question answering of VQA, the conventional 2D-QA models suffer from problems with spatial understanding of object alignment and directions and fail the object localization from the textual questions in 3D-QA. We propose a baseline model for 3D-QA, named ScanQA model, where the model learns a fused descriptor from 3D object proposals and encoded sentence embeddings. This learned descriptor correlates the language expressions with the underlying geometric features of the 3D scan and facilitates the regression of 3D bounding boxes to determine described objects in textual questions. We collected human-edited question-answer pairs with free-form answers that are grounded to 3D objects in each 3D scene. Our new ScanQA dataset contains over 41K question-answer pairs from the 800 indoor scenes drawn from the ScanNet dataset. To the best of our knowledge, ScanQA is the first large-scale effort to perform object-grounded question-answering in 3D environments.

1. Introduction

In recent years, there are great advances in vision-and-language tasks and datasets, and a number of new datasets are created to develop models that understand textual expressions, such as captions or questions, that are grounded to 2D images, such as image captioning [12, 40], understanding of referring expressions [24, 48], image region and phrase correspondence [35], and visual question answering (VQA) [6, 19, 22]. VQA is successful to grasp object natures that are visualized in 2D frames. However, when we develop models that understand spatial information of 3D scenes, such as “What is between the table and TV set?” or “Where is the suitcase located?”, existing models based

* denotes equally contributed.

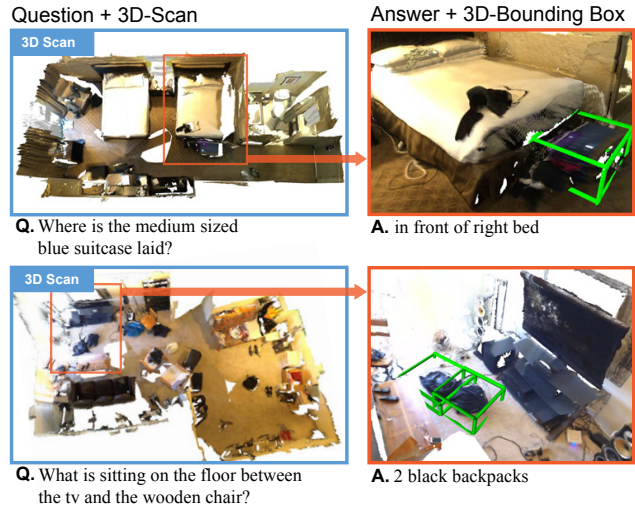


Figure 1. We introduce the new task of question answering for 3D modeling. Give inputs of the entire 3D modeling and a linguistic question, models predict an answer phrase and corresponding 3D-bounding boxes.

on 2D images have several issues to have accurate understandings of the 3D world. For example, 2D images lack of the accurate sense of the relative directions and distances in the original 3D scenes, i.e., the stereoscopic attribute perception problem. The object in question can be hidden by other objects when they overlap, i.e., the occlusion problem. When multiple images are used in the 2D-image based question answering models, such models often face difficulties to track and recognize whether some objects are the same object between images or not, i.e., the object localization and identification problem.

Currently, it becomes possible to develop 3D spatial understanding models for 3D object localization task of ScanRefer [10], dialog-based localization of ReferIt3D [1] and 3D object captioning task of Scan2cap [13]. Embodied Question Answering [17, 44, 47] is one of significant tasks to navigate agents in the 3D scene given some question. We believe that 3D spatial understanding datasets contribute to developing models that comprehend the embodied 3D scene, and ask and answer questions about the 3D environment as humans do. However, unlike its 2D image

counterpart, the question answering datasets on 3D environmental annotations are still limited in terms of dataset size and question variety because existing datasets often rely on template-based question-answer collections.

In this paper, we propose a 3D Question Answering (3D-QA) task, using 3D spatial information instead of 2D images to comprehend real world information through the question answering form. In 3D-QA task, models answer a question given the 3D scene along with the object localization described in the question. We present the overview of the task in Fig. 1. This 3D-QA task setting is reasonable when external sensors or mobile robots collect the sufficient visual information to construct a 3D scene prior to the QA task. We assume this is plausible when the model can use the preliminary captured visual information from the 3D scene due to the prior navigation in the scene, such as vision-and-language navigation [5]. This task is also applicable to real-world services that use preliminary extracted 3D scenes such as interactive virtual room viewing services or searching in indoor scenes.

For 3D-QA task, we developed a novel ScanQA dataset, which is based on RGB-D scans of the indoor scene and annotations drawn from the ScanNet dataset [15]. We automatically generated questions from object captions of ScanRefer [10] with question generation models. However, these auto-generated questions included many invalid questions and therefore we filtered the invalid questions and refined the questions if necessary. We further collect free-form answers and object annotations from humans with a newly developed interactive 3D scene viewer. In total, we gathered 41k question-answer pairs with 32k unique questions. We propose a 3D-QA model with a textual and 3D scene encoding and several baseline models including 2D image models (2D-QA) and the combination of 3D object localization model [10, 36] and question answering model [49]. We confirmed that the ScanQA model outperformed these baseline models in most of the evaluations including exact matching and image captioning metrics in the proposed ScanQA dataset.

2. Related work

The 3D-QA task has close relations to existing visual question answering and 3D embodied question answering. We place our task as a spatial comprehension of the entire 3D scene given linguistic questions.

2.1. Visual Question Answering

Visual Question Answering is a task in which models are given a 2D image and a question about its content. Then, they are expected to give an appropriate answer. Question answering in 2D images was proposed by Malinowski *et al.* [32], and various inference methods [4, 6, 49] have been proposed since then. One of the best VQA methods is Os-

car [28], which uses Mask R-CNN to infer the solution by considering the relation between individual objects in the image. In addition, Jang *et al.* [23] proposed a question answering method that takes into account more detailed vision information and motion information by using video. ClipBERT [27] improved the accuracy by dividing the video into clips and letting them reason individually. VQA on 360° [14] is a task to answer questions about a 360° image. Although VQA on 360° contribute to understand the 3D scene, the available information is limited compared to the ScanQA dataset. Our dataset also include the object identification task which is different from the existing dataset of VQA on 360°.

2.2. 3D Object Localization with Language

ScanRefer [10] is a task to localize an object referred in a free-form text description. The ScanRefer model identifies a 3D-bounding box for an object given the input description. This dataset is based on 800 scenes drawn from ScanNet dataset [15]. In addition to question answering on 3D scenes, the 3D-QA task also includes the object localization task for objects that appear in the question answering. Unlike the ScanRefer task, the objects in the ScanQA object localization can be multiple because multiple objects can appear in a single question.

2.3. Question Answering in 3D scenes

Unlike 2D-QA, for which many datasets have been proposed, 3D question answering datasets are still limited. We notice that the existing question answering tasks on 3D scenes take interactive forms. The interactive QA dataset (IQUAD) [18] on AI2THOR [26] allows model-agents to interact with objects in the scene to find the answer to the question. Embodied question answering (EQA) [17, 44, 47] is the combination of VQA and vision-and-language navigation task [5, 11, 41, 45]. In the original EQA dataset [17], the embodied model-agent receives a question such as “What color is the car?” and navigates to the described object in the question in House 3D [45]. MP3D-EQA [44] is the photorealistic embodied QA on Matterport 3D scans [9]. MT-EQA [47] is the multi-target variations of EQA. We summarize the relation of these datasets to ScanQA in Table 1. Unlike these datasets, ScanQA dataset is not created from fixed templates and hence includes more natural and a much larger number of unique questions as discussed in Sec. 3.3.

3. ScanQA Dataset

We hereby define the 3D-QA task and describe the collection of the corresponding dataset.

3D-QA datasets	Type	Question Collection	Answer Collection	Environment	Photorealistic	# 3D Scenes
IQUAD	Interactive	Template-based	Template-based	AI2THOR	No	30 rooms
EQA	Navigation	Template-based	Template-based	House3D	No	588 scenes
MP3D-EQA	Navigation	Template-based	Template-based	Matterport 3D	Yes	144 floors
MT-EQA	Navigation	Template-based	Template-based	House3D	No	588 scenes
Scan QA dataset	3D Scan	AutoGen+HumanEdit	Human	ScanNet	Yes	800 rooms

Table 1. Comparison of 3D question-answering datasets.

3.1. 3D-QA Task

As illustrated in Fig. 1, 3D-QA task requires models to answer a question given a entire information of the 3D scene. Here, models use the 3D spatial information, such as RGB-D scans or point cloud data. We also require models to specify 3D-bounding boxes of the objects that are related to this question-answering. This prevents models from answering to questions relying on textual priors of the trained questions and without looking at the scene. However, unlike the ScanRefer dataset, we do not require models to determine one described object for each question. This is because multiple objects can be utilized to answer some questions. For example, a question “What color is the chairs around the table?” are related to multiple objects. This question is also answerable as long as the chairs around the unique table in the scene have the same color. In such cases, we require models to determine multiple 3D-bounding boxes in addition to answering the question.

3.2. Question-Answer Collection

The ScanQA dataset was created in multiple phrases: automatic QA generation [2, 8, 30, 46], question filtering, question editing, and answer collection. First, we automatically generate question-answer pairs from the captions to identify objects in 3D scenes drawn from the ScanRefer dataset [10]. We applied the question and answer generation model based on a T5-base model [38] trained on a text-based question answering dataset [39]¹ for the ScanRefer captions and obtained the seed questions. However, these autogenerated question-answer pairs include many inadequate questions, such as questions that are underspecified or not grounded to the scene as presented in Fig. 2. Auto-generated questions also include too easy questions that can be answered with common sense. Therefore, we decide to remove such questions as much as possible. We also generated an auto-generated answer for each question. However, we decided not to include such auto-generated answers in the final dataset because it is not sure that they are grounded to scenes. We therefore applied filtering and editing for the seed questions in addition to the answer collection using Amazon Mechanical Turk. We developed an interactive vi-

¹We used the weights available at <https://huggingface.co/valhalla/t5-base-qa-qg-hl>.

Split	# Question	# Unique question	# 3D Scenes
Train	25,563	20,546	562
Val	4,675	4,306	71
Test w/ objects	4,976	4,552	70
Test w/o objects	6,149	5,484	97
Total	41,363	32,337	800

Table 2. ScanQA dataset statistics.

sualization website for each 3D scan that allows workers to rotate the 3D scene and check the object names and IDs if they are available. Following the ScanRefer dataset, we attach the object names and IDs for objects in the 3D scene. We embedded this visualization site into AMT task page as presented in Fig. 2.

Filtering and editing of the seed questions works as follows. We first filtered inadequate questions from the auto-generated seed questions by basic rules. We then asked workers to classify the remaining questions into four classes: *valid*, *too easy*, *unanswerable* and *unclear* questions. Each question was classified by at least three workers. We chose the questions that two or more workers marked as valid for the next phrase of the editing and answer collection process. In the editing and answer collection process, we presented filtered questions to workers and firstly asked them to rewrite the questions themselves if they are inadequate for the scene. Finally, workers wrote down free-form answers to the questions. We also collect the object IDs that are used in question to identify the object in the scene in this phrase.

3.3. Dataset Statistics

In total, we collected 41,363 questions and 58,191 answers, including 32,337 unique questions and 16,999 unique answers. Table 2 presents the statistics of the ScanQA dataset. This is in order of magnitude larger than existing embodied question answering datasets in terms of both question size and variations. For example, the EQA dataset [17] contains 4,246 questions that consists of 147 unique questions in its training set. The EQA-MP3D dataset [44] includes 767 questions consists of 174 unique questions in its training set. Considering that our dataset contains not only question-answer pairs but also 3D ob-

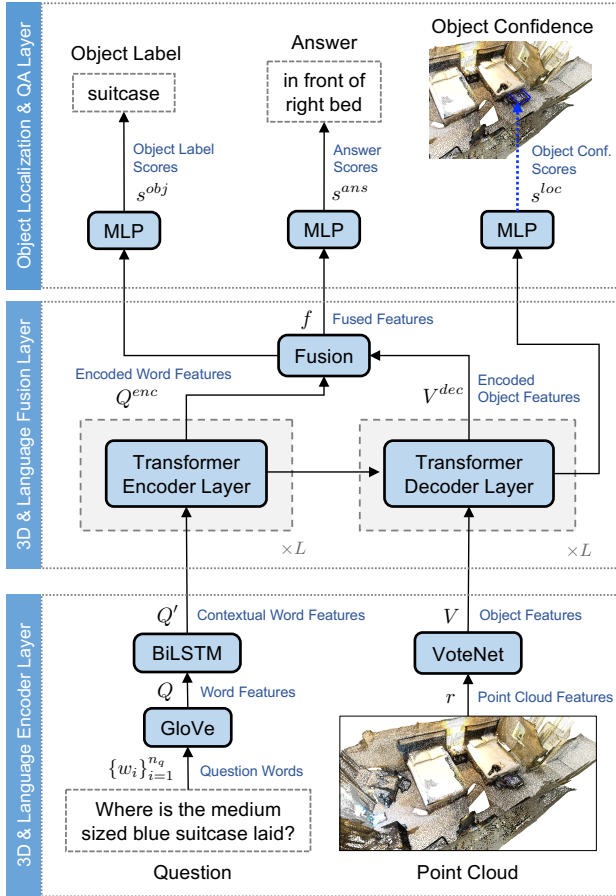


Figure 4. Illustration of our ScanQA model for answering 3D environments. Given point cloud and RGB frame sequence that capture indoor scenes, the QA model outputs a corresponding answer by fusing 3D and language information through three layers such as 3D scene and language encoder layer, fusion layer, classification layers.

as a backbone network. We obtain the object proposals (object boxes) from VoteNet and project them using a nonlinear layer with GELUs activation to obtain the object proposal representation $V \in \mathbb{R}^{n_v \times d}$, where n_v is the number of object proposals (set to 256.)

3D & language fusion layer. Inspired by the architecture of the deep modular co-attention networks of MCAN [49], often used for VQA, we use transformer blocks [42] to represent the relationships between object proposals and between question words. After feeding contextual question representation Q' into a stack of L (set to two) transformer encoder layers, we obtain deeply contextualized question representation $Q^{enc} \in \mathbb{R}^{n_q \times d}$. In addition, we use transformer decoder layers to represent the features of object proposals related to the question words by using the final output of the transformer encoder as decoder’s keys and values. We obtain a question-aware-object proposal repre-

sentation $V^{dec} \in \mathbb{R}^{n_v \times d}$ after feeding question and object proposal pairs into a stack of L transformer decoder layers. Then, the final outputs of transformer layers Q^{enc} and V^{dec} are fused by a fusion layer that uses a two-layer multi-layer perceptron (MLP) with attention mechanism [31] (see details [49].) We obtain the fused feature $f \in \mathbb{R}^d$ that simultaneously represents 3D scene and linguistic question information.

Object localization & QA layer. This layer consists of object localization, object classification, and answer classification modules. The description of each module is as follows.

Object localization module aims to predict which of the proposed object boxes corresponds to the question. The question-aware-object proposal representation $V^{dec} \in \mathbb{R}^{n_v \times d}$ is fed into a two-layer MLP to determine how likely each object box is related to the question. Following [10], we compute the localization confidences $s^{loc} \in \mathbb{R}^{n_v}$ for the proposed n_v object boxes with a softmax function and use cross-entropy (CE) loss to train this module.

Object classification module predicts what objects are associated with a question. Note that many questions do not contain target object names related to the answer in contrast to the 3D localization task [10, 50, 51]. We use the 3D and question-aware fused feature f and feed it into a two-layer MLP to predict 18 ScanNet benchmark classes. We compute the object classification scores $s^{obj} \in \mathbb{R}^{18}$ with a softmax function and use CE loss to train this module.

Answer classification module predicts an answer corresponding the question and scene. We project the fused feature f into a vector $s^{ans} \in \mathbb{R}^{n_a}$ for the n_a answer candidates in the training set. To consider multiple answers, we compute final scores normalized by a sigmoid function and use binary cross-entropy (BCE) as the loss function to train this module.

Loss function. We use a loss function similar to ScanRefer [10], such as localization loss \mathcal{L}_{loc} of the object localization module, object detection loss \mathcal{L}_{det} of the VoteNet [36], and object classification loss \mathcal{L}_{obj} of the object classification module. For answering 3D scene content, we additionally use an answer loss \mathcal{L}_{ans} of the answer classification module. We set the final loss a simple linear combination of these losses computed as $\mathcal{L} = \mathcal{L}_{ans} + \mathcal{L}_{obj} + \mathcal{L}_{loc} + \mathcal{L}_{det}$.

5. Experiments

5.1. Experimental Setup

In this experimental setup, we refer to the experimental setup of existing studies on scene understanding of ScanNet [15] through languages such as ScanRefer and Scan2Cap [10, 13].

Data augmentation. We apply data augmentation to our training data and apply rotation about all three axes by a

Model	EM@1	EM@10	BLEU-1	BLEU-2	BLEU-3	BLEU-4	ROUGE	METEOR	CIDEr	SPICE
Test w/ objects										
RandomImage+MCAN	22.31	53.11	26.66	18.49	16.16	14.26	31.27	12.13	60.37	9.05
VoteNet+MCAN	19.71	50.76	29.46	17.23	10.33	6.08	30.97	12.07	58.23	10.44
ScanRefer+MCAN (pipeline)	17.52	49.92	19.17	10.66	0.00	0.00	24.40	9.38	44.25	6.24
ScanRefer+MCAN (e2e)	20.56	52.35	27.85	17.27	11.88	7.46	30.68	11.97	57.36	10.58
ScanQA	23.45	56.51	31.56	21.39	15.87	12.04	34.34	13.55	67.29	11.99
Test w/o objects										
RandomImage+MCAN	20.82	51.23	26.29	17.90	14.27	9.66	29.23	11.54	55.64	8.87
VoteNet+MCAN	18.15	48.56	29.63	17.80	11.57	7.10	29.12	11.68	53.34	10.36
ScanRefer+MCAN (pipeline)	16.47	49.05	18.71	10.98	16.53	0.76	22.45	8.76	40.81	6.41
ScanRefer+MCAN (e2e)	19.04	49.70	26.98	16.17	11.28	7.82	28.61	11.38	53.41	10.63
ScanQA	20.90	54.11	30.68	21.20	15.81	10.75	31.09	12.59	60.24	11.29

Table 3. Performance comparison for question answering with image captioning metrics. **e2e** represents an end-to-end model.

ANS	OBJ	LOC	EM@1	EM@10	BLEU-1	BLEU-2	BLEU-3	BLEU-4	ROUGE	METEOR	CIDEr	SPICE
Test w/ objects												
✓			12.16	42.77	12.86	5.45	0.12	0.02	17.55	6.71	29.17	4.05
✓	✓		18.31	49.18	22.32	14.53	11.15	7.92	26.37	9.94	49.10	6.36
✓		✓	20.46	51.67	25.06	16.91	14.06	11.37	29.22	11.13	55.17	8.21
✓	✓	✓	23.45	56.51	31.56	21.39	15.87	12.04	34.34	13.55	67.29	11.99
Test w/o objects												
✓			10.78	39.44	11.94	5.02	0.12	0.02	15.34	5.91	25.51	3.51
✓	✓		16.23	46.30	21.37	13.49	10.71	7.64	23.63	9.10	43.21	6.13
✓		✓	18.12	49.60	25.12	17.58	14.68	10.23	26.50	10.43	49.93	8.16
✓	✓	✓	20.90	54.11	30.68	21.20	15.81	10.75	31.09	12.59	60.24	11.29

Table 4. Performance comparison between the different experimental conditions of the ScanQA model.

Model	Acc@0.25	EM@10
Test w/ objects		
ScanQA (xyz)	23.67	55.67
ScanQA (xyz+rgb)	23.45	55.43
ScanQA (xyz+rgb+normal)	23.35	54.50
ScanQA (xyz+multiview)	25.40	55.51
ScanQA (xyz+multiview+normal)	25.44	56.51

Table 5. Feature ablation results

random angle in $[-5^\circ, 5^\circ]$ and randomly translate the point cloud within 0.5 meters in all directions. Since the ground alignment in ScanNet is incomplete, we rotate it on all axes (not just the top).

Training. For training ScanQA model, we used Adam [25], batch size 16, and an initial learning rate of $5e-4$. We trained the model for 30 epochs until converge and decreased the learning rate by 0.2 times after 15 epochs. To mitigate fitting the model exactly against its training data, we set the weight decay factor to $1e-5$.

Evaluation. To evaluate QA performance, we used exact matches EM@1 and EM@10 as the evaluation metric, where EM@K is the percentage of predictions in which the top K predicted answers exactly match any one of the ground-truth answers. We also include sentence evaluation

metrics frequently used for image captioning models because some of the questions have multiple possible answer expressions, as discussed in Sec. 3.3. We add BLEU [33], ROUGE-L [29], METEOR [7], CIDEr [43] and SPICE [3] metrics for the evaluation of robust answer matching.

Baselines. To validate our 3D-QA model (ScanQA), we prepared several baselines. The empirical experiments were conducted using the following methods.

RandomImage+2D-QA First, we prepared several 2D-QA models as baselines to demonstrate how our 3D-QA models outperform 2D-based VQA models for the 3D-QA task. We used a pre-trained MCAN model [49] as a 2D-QA model. MCAN is a transformer network [42] that uses the cross attention mechanism to represent the relationship between question words and objects in the image. The proposed method uses some of the modules used in MCAN, such as transformer encoder and decoder layers, to create 3D and language features. By comparing the two, we can confirm the importance of creating a model specialized for 3D-QA. Since 2D-QA models cannot be directly applied to a 3D environment, we randomly sampled three images from the video taken to build the ScanNet dataset. We used a bottom-up top-down attention model [4] for extracting objects' appearance features. We applied pretrained 2D-QA models to

these images and computed the answer score for each image. Finally, we select the most probable answer according to these images’ averaged all answer scores. We experiment with 2D-QA by using three images taken in the environment per question.

OracleImage+2D-QA To investigate the upper bound on the performance of 2D-QA for questions in 3D space, we used images around a target object associated with a question-answer pair. We set the camera’s position based on the coordinates of the bounding box of the correct object and take images from the direction and distance where the bounding box is most visible. Since the object may not be visible depending on the camera’s position, we use three images per question. We applied 2D-QA models to these images similar to RandomImage+2D-QA. Note that it is difficult to obtain such images in actual QA situations. By looking at the performance of this method, we can learn the difficulty in solving the 3D-QA task using 2D-QA models.

VoteNet+MCAN VoteNet [36] is a 3D object detection method for locating and recognizing objects in a 3D scene. This method detects objects in 3D space, extracts their features, and uses them in a standard VQA model (MCAN). Unlike our method, this method does not consider where the target object is located in the 3D space or what the target object is.

ScanRefer+MCAN (pipeline) ScanRefer [10] is a 3D object localization method for localizing a given linguistic description to a corresponding target object in 3D space. ScanRefer internally uses VoteNet to detect objects in the room and estimates the object corresponding to the linguistic description from among the candidate objects. Note that ScanRefer cannot be used directly for QA. Thus, we used a pre-trained ScanRefer model (using the same features that our model used) to identify the object corresponding to the question and then applied 2D-QA (MCAN) to the image surrounding the object localized by ScanRefer. Note that ScanRefer and MCAN are run separately, end-to-end learning is not possible.

ScanRefer+MCAN (end-to-end) This method is more sophisticated and closer to the proposed method. While ScanRefer+MCAN (pipeline) conducts the object localization and QA separately, this method simultaneously learns localization and QA modules. Specifically, the method takes as input the object proposal feature of ScanRefer for VQA models and then predicts answers based on object box features and question content. Unlike the ScanQA model, this uses the output of VoteNet separately for object localization and QA modules (even though the information for both tasks is helpful for each other) and does not learn both modules in common.

5.2. Quantitative Analysis

The performance of 3D-QA on the ScanQA dataset is shown in Table 3, along with the image caption metrics. The best results in each column are shown in bold. We compared our ScanQA model with the competitive baselines: VoteNet+MCAN, ScanRefer+MCAN (pipeline), and ScanRefer+MCAN (end-to-end). These baselines share some of the proposed method’s components and help us understand which components are useful for 3D-QA. The results show that our ScanQA method significantly outperformed all baselines across all data splits over all evaluation metrics. In particular, ScanQA significantly outperformed ScanRefer+MCAN (end-to-end), which learns QA and object localization separately across all data splits over all evaluation metrics, indicating that the ScanQA model has succeeded in synergistic learning by sharing object localization and QA module. ScanQA also outperformed VoteNet+MCAN with large margins. This result suggests using object localization in 3D space and predicting object categories that are related to questions are important for 3D-QA. We will clarify this point in the ablation study. Interestingly, VoteNet+MCAN, ScanRefer+MCAN (end-to-end), ScanQA markedly outperformed ScanRefer+MCAN (pipeline), which detect target objects related to a question using a pretrained ScanRefer and then apply 2D-QA to surrounding images of a target object. The results indicate that end-to-end training with 3D and language information is suitable for solving 3D-QA model problems. In addition, we observed our 3D-QA model, ScanQA, is superior to a 2D-QA model, RandomImage+MCAN, which uses a powerful pre-trained model. We also notice that 2D-QA baseline with oracle object identification of OracleImage+MCAN performs better or competitive than the ScanQA model. Although this suggests that accurate object identification for the questions surely boosts 3D-QA results, this is an oracle setting for real world applications.

5.3. Ablation Studies

In this section, we conduct ablation studies concerning ScanQA model’s design. The effect of each major component of the proposed method is shown in Table 4, and the effect of different input data is shown in Table 5.

Does object classification help? We show how object classification is effective by conducting an experiment of ScanQA combined with and without the object classification module. We compare our method trained with the answer and object classification modules (ANS+OBJ) with a model trained with only the answer module (ANS) and also compare a model trained with full modules (ANS+OBJ+LOC) with one trained with the answer and object localization modules (ANS+LOC). The results in Table 4 presents that the models with OBJ outperformed others. This suggests that predicting the category of the target

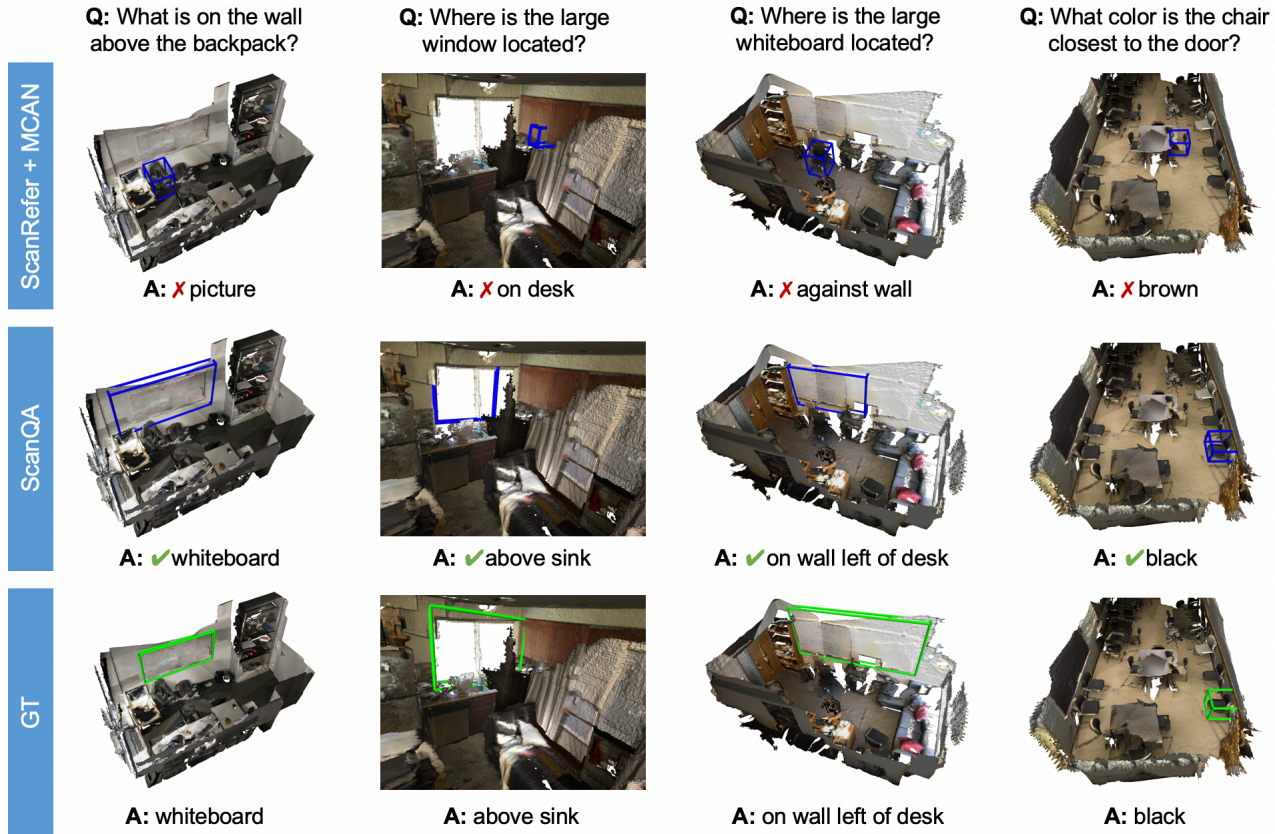


Figure 5. **Qualitative results.** Predicted answers are described below each figure. Predicted boxes are marked blue and ground truth are marked green. We show examples where ScanQA produced good object localization when predicting correct answers while ScanRefer+MCAN (pipeline) could not.

object is effective for 3D-QA.

Does object localization help? We show how object localization is effective by conducting an experiment ScanQA + the object localization module and without. We compare our method trained with the answer and object localization modules (ANS+LOC) with a model trained with only the answer module (ANS) and also compare a model trained with full modules (ANS+OBJ+LOC) with one trained with the answer and object classification modules (ANS+OBJ). The results in Table 4 show that the model with LOC consistently outperformed others. This suggests that localizing target objects is also important to improve 3D-QA performance.

Do colors help for 3D-QA? According to the ScanRefer study, models that use color information have better object localization performance than models that use only geometry [10]. Motivated by this finding, we also evaluate several models using different features. We compare our method trained with the geometry (xyz) and multiview image features (xyz+multiview) with a model trained with only geometry (xyz) and one trained with RGB values from the reconstructed meshes (xyz+rgb). To validate object localiza-

tion performance, we use accuracy (Acc@0.25), where the positive predictions have a higher intersection over union with the ground truths than the threshold 0.25 used in [10]. From Table 5, we found RGB values are not effective for both object localization and QA. The multiview image features are slightly effective for object localization but not on QA. The result is because the ScanQA dataset is more difficult to associate language and object information than the ScanRefer dataset, since multiple objects may apply to a single question. Fortunately, ScanQA trained with geometry, pre-processed multiview image features and normals outperforms others, but the effect was limited. This result suggests that subsequent studies should consider a more balanced selection of features regarding computational cost and performance.

5.4. Qualitative Analysis

Finally, we demonstrate how well our model works by visualizing qualitative examples of ScanQA, ScanRefer+MCAN (pipeline), and the ground truth (GT). Fig. 5 shows the representative QA results of a baseline method and ScanQA. The results suggest that answering the ques-

tions requires object localization related to the answer according to question content and point cloud matching. For example, the leftmost case shows a whiteboard is located above a backpack, which could not be answered by ScanRefer+MCAN (pipeline) that localized the backpack in error. The reason is that the QA module and the localization module are separated in ScanRefer+MCAN (pipeline). In contrast, our model successfully localized target objects related to answers and predicted correct answers by simultaneously learning QA and object localization.

6. Conclusion

Spatial understanding with language expression is a core technology for models that are deployed in the real world and interact with humans. We introduce a novel task of 3D question answering (3D-QA), where models observe an entire 3D scan and answer the question about the 3D modeling in addition to the object localization. For this task, we create a new dataset of ScanQA based on the ScanRefer dataset. ScanQA dataset consists of 41,363 questions and 32,337 unique answers from 800 scenes drawn from the ScanNet scenes. We propose a 3D-QA baseline model of ScanQA. We confirm that the ScanQA baseline performs better than the counterpart of 2D-based VQA baselines in most of the evaluation measures including the exact match and image captioning metrics.

References

- [1] Panos Achlioptas, Ahmed Abdelreheem, Fei Xia, Mohamed Elhoseiny, and Leonidas J. Guibas. ReferIt3D: Neural listeners for fine-grained 3d object identification in real-world scenes. In *Proceedings of the 16th European Conference on Computer Vision (ECCV)*, 2020. 1
- [2] Chris Alberti, Daniel Andor, Emily Pitler, Jacob Devlin, and Michael Collins. Synthetic QA corpora generation with roundtrip consistency. In *Proceedings of the 57th Annual Meeting of the Association for Computational Linguistics (ACL)*, pages 6168–6173, 2019. 3
- [3] Peter Anderson, Basura Fernando, Mark Johnson, and Stephen Gould. SPICE: Semantic propositional image caption evaluation. In *Proceedings of the European Conference on Computer Vision (ECCV)*, 2016. 6
- [4] Peter Anderson, Xiaodong He, Chris Buehler, Damien Teney, Mark Johnson, Stephen Gould, and Lei Zhang. Bottom-up and top-down attention for image captioning and visual question answering. In *Proceedings of the IEEE/CVF Conference on Computer Vision and Pattern Recognition (CVPR)*, 2018. 2, 6
- [5] Peter Anderson, Qi Wu, Damien Teney, Jake Bruce, Mark Johnson, Niko Sünderhauf, Ian Reid, Stephen Gould, and Anton van den Hengel. Vision-and-Language Navigation: Interpreting visually-grounded navigation instructions in real environments. In *Proceedings of the IEEE/CVF Conference on Computer Vision and Pattern Recognition (CVPR)*, 2018. 2
- [6] Stanislaw Antol, Aishwarya Agrawal, Jiasen Lu, Margaret Mitchell, Dhruv Batra, C. Lawrence Zitnick, and Devi Parikh. VQA: Visual Question Answering. In *Proceedings of the IEEE/CVF International Conference on Computer Vision (ICCV)*, 2015. 1, 2
- [7] Satyanjeev Banerjee and Alon Lavie. METEOR: An automatic metric for MT evaluation with improved correlation with human judgments. In *Proceedings of the ACL Workshop on Intrinsic and Extrinsic Evaluation Measures for Machine Translation and/or Summarization*. Association for Computational Linguistics, 2005. 6
- [8] Ying-Hong Chan and Yao-Chung Fan. A recurrent BERT-based model for question generation. In *Proceedings of the 2nd Workshop on Machine Reading for Question Answering*, 2019. 3
- [9] Angel Chang, Angela Dai, Thomas Funkhouser, Maciej Halber, Matthias Niessner, Manolis Savva, Shuran Song, Andy Zeng, and Yinda Zhang. Matterport3D: Learning from RGB-D data in indoor environments. *International Conference on 3D Vision (3DV)*, 2017. 2
- [10] Dave Zhenyu Chen, Angel X Chang, and Matthias Nießner. Scanrefer: 3d object localization in rgb-d scans using natural language. In *Proceedings of the European Conference on Computer Vision (ECCV)*. Springer, 2020. 1, 2, 3, 4, 5, 7, 8
- [11] Howard Chen, Alane Suhr, Dipendra Misra, Noah Snaveley, and Yoav Artzi. Touchdown: Natural language navigation and spatial reasoning in visual street environments. In *Proceedings of the IEEE/CVF Conference on Computer Vision and Pattern Recognition (CVPR)*, 2019. 2
- [12] Xinlei Chen, Hao Fang, Tsung-Yi Lin, Ramakrishna Vedantam, Saurabh Gupta, Piotr Dollár, and C. Lawrence Zitnick. Microsoft coco captions: Data collection and evaluation server. *CoRR*, abs/1504.00325, 2015. 1
- [13] Zhenyu Chen, Ali Gholami, Matthias Nießner, and Angel X Chang. Scan2cap: Context-aware dense captioning in rgb-d scans. In *Proceedings of the IEEE/CVF Conference on Computer Vision and Pattern Recognition (CVPR)*, 2021. 1, 4, 5
- [14] Shih-Han Chou, Wei-Lun Chao, Wei-Sheng Lai, Min Sun, and Ming-Hsuan Yang. Visual question answering on 360deg images. In *Proceedings of the IEEE/CVF Winter Conference on Applications of Computer Vision (WACV)*, 2020. 2
- [15] Angela Dai, Angel X Chang, Manolis Savva, Maciej Halber, Thomas Funkhouser, and Matthias Nießner. Scannet: Richly-annotated 3d reconstructions of indoor scenes. In *Proceedings of the IEEE/CVF Conference on Computer Vision and Pattern Recognition (CVPR)*, 2017. 2, 5
- [16] Angela Dai and Matthias Nießner. 3DMV: Joint 3d-multi-view prediction for 3d semantic scene segmentation. In *Proceedings of the European Conference on Computer Vision (ECCV)*, 2018. 4
- [17] Abhishek Das, Samyak Datta, Georgia Gkioxari, Stefan Lee, Devi Parikh, and Dhruv Batra. Embodied Question Answering. In *Proceedings of the IEEE/CVF Conference on Computer Vision and Pattern Recognition (CVPR)*, 2018. 1, 2, 3

- [18] Daniel Gordon, Aniruddha Kembhavi, Mohammad Rastegari, Joseph Redmon, Dieter Fox, and Ali Farhadi. IQA: Visual question answering in interactive environments. In *Proceedings of the IEEE/CVF Conference on Computer Vision and Pattern Recognition (CVPR)*. IEEE, 2018. 2
- [19] Yash Goyal, Tejas Khot, Douglas Summers-Stay, Dhruv Batra, and Devi Parikh. Making the v in vqa matter: Elevating the role of image understanding in visual question answering. In *Proceedings of the IEEE Conference on Computer Vision and Pattern Recognition (CVPR)*, July 2017. 1
- [20] Dan Hendrycks and Kevin Gimpel. Gaussian error linear units (GELUs). *CoRR*, abs/1606.08415, 2016. 4
- [21] Sepp Hochreiter and Jürgen Schmidhuber. Long short-term memory. *Neural computation*, 9(8):1735–1780, 1997. 4
- [22] Drew A Hudson and Christopher D Manning. Gqa: A new dataset for real-world visual reasoning and compositional question answering. *Proceedings of the IEEE/CVF Conference on Computer Vision and Pattern Recognition (CVPR)*, 2019. 1
- [23] Yunseok Jang, Yale Song, Chris Dongjoo Kim, Youngjae Yu, Youngjin Kim, and Gunhee Kim. Video Question Answering with Spatio-Temporal Reasoning. *International Journal of Computer Vision (IJCV)*, 2019. 2
- [24] Sahar Kazemzadeh, Vicente Ordonez, Mark Matten, and Tamara Berg. ReferItGame: Referring to objects in photographs of natural scenes. In *Proceedings of the 2014 Conference on Empirical Methods in Natural Language Processing (EMNLP)*, pages 787–798, Doha, Qatar, 2014. Association for Computational Linguistics. 1
- [25] Diederik Kingma and Jimmy Ba. Adam: A method for stochastic optimization. In *Proceedings of the International Conference on Learning Representations (ICLR)*, 2015. 6
- [26] Eric Kolve, Roozbeh Mottaghi, Winson Han, Eli VanderBilt, Luca Weihs, Alvaro Herrasti, Daniel Gordon, Yuke Zhu, Abhinav Gupta, and Ali Farhadi. AI2-THOR: An Interactive 3D Environment for Visual AI. *arXiv*, 2017. 2
- [27] Jie Lei, Linjie Li, Luowei Zhou, Zhe Gan, Tamara L. Berg, Mohit Bansal, and Jingjing Liu. Less is more: ClipBERT for video-and-language learning via sparse sampling. In *Proceedings of the IEEE/CVF Conference on Computer Vision and Pattern Recognition (CVPR)*, 2021. 2
- [28] Xiujun Li, Xi Yin, Chunyuan Li, Xiaowei Hu, Pengchuan Zhang, Lei Zhang, Lijuan Wang, Houdong Hu, Li Dong, Furu Wei, Yejin Choi, and Jianfeng Gao. Oscar: Object-semantic aligned pre-training for vision-language tasks. *Proceedings of the European Conference on Computer Vision (ECCV)*, 2020. 2, 1
- [29] Chin-Yew Lin. ROUGE: A package for automatic evaluation of summaries. In *Text Summarization Branches Out*, pages 74–81. Association for Computational Linguistics, 2004. 6
- [30] Luis Enrico Lopez, Diane Kathryn Cruz, Jan Christian Blaise Cruz, and Charibeth Cheng. Simplifying paragraph-level question generation via transformer language models. In Duc Nghia Pham, Thanaruk Theeramunkong, Guido Governatori, and Fenrong Liu, editors, *Proceedings of the Pacific Rim International Conference on Artificial Intelligence (PRICAI)*, 2021. 3
- [31] Thang Luong, Hieu Pham, and Christopher D. Manning. Effective approaches to attention-based neural machine translation. In *Proceedings of the Empirical Methods in Natural Language Processing (EMNLP)*, pages 1412–1421, 2015. 5
- [32] Mateusz Malinowski and Mario Fritz. A multi-world approach to question answering about real-world scenes based on uncertain input. In *Proceedings of the Neural Information Processing Systems (NeurIPS)*, 2014. 2
- [33] Kishore Papineni, Salim Roukos, Todd Ward, and Wei-Jing Zhu. Bleu: a method for automatic evaluation of machine translation. In *Proceedings of the 40th Annual Meeting of the Association for Computational Linguistics (ACL)*, pages 311–318, Philadelphia, Pennsylvania, USA, 2002. Association for Computational Linguistics. 6
- [34] Jeffrey Pennington, Richard Socher, and Christopher D Manning. GloVe: Global vectors for word representation. In *Proceeding of Empirical Methods in Natural Language Processing (EMNLP)*, 2014. 4
- [35] B. A. Plummer, L. Wang, C. M. Cervantes, J. C. Caicedo, J. Hockenmaier, and S. Lazebnik. Flickr30k entities: Collecting region-to-phrase correspondences for richer image-to-sentence models. In *Proceedings of the IEEE/CVF International Conference on Computer Vision (ICCV)*, pages 2641–2649, 2015. 1
- [36] Charles R. Qi, Or Litany, Kaiming He, and Leonidas J. Guibas. Deep hough voting for 3d object detection in point clouds. In *Proceedings of the IEEE/CVF International Conference on Computer Vision (ICCV)*, 2019. 2, 4, 5, 7
- [37] Charles Ruizhongtai Qi, Li Yi, Hao Su, and Leonidas J Guibas. PointNet++: Deep hierarchical feature learning on point sets in a metric space. In *Proceedings of Neural Information Processing Systems (NeurIPS)*, 2017. 4
- [38] Colin Raffel, Noam Shazeer, Adam Roberts, Katherine Lee, Sharan Narang, Michael Matena, Yanqi Zhou, Wei Li, and Peter J. Liu. Exploring the limits of transfer learning with a unified text-to-text transformer. *Journal of Machine Learning Research*, 21(140):1–67, 2020. 3
- [39] Pranav Rajpurkar, Jian Zhang, Konstantin Lopyrev, and Percy Liang. SQuAD: 100,000+ questions for machine comprehension of text. In *Proceedings of the 2016 Conference on Empirical Methods in Natural Language Processing (EMNLP)*, 2016. 3
- [40] Piyush Sharma, Nan Ding, Sebastian Goodman, and Radu Soricut. Conceptual captions: A cleaned, hypernymed, image alt-text dataset for automatic image captioning. In *Proceedings of the Association for Computational Linguistics (ACL)*, 2018. 1
- [41] Mohit Shridhar, Jesse Thomason, Daniel Gordon, Yonatan Bisk, Winson Han, Roozbeh Mottaghi, Luke Zettlemoyer, and Dieter Fox. ALFRED: A Benchmark for Interpreting Grounded Instructions for Everyday Tasks. In *Proceedings of The IEEE/CVF Conference on Computer Vision and Pattern Recognition (CVPR)*, 2020. 2
- [42] Ashish Vaswani, Noam Shazeer, Niki Parmar, Jakob Uszkoreit, Llion Jones, Aidan N Gomez, Łukasz Kaiser, and Illia Polosukhin. Attention is all you need. In I. Guyon, U. V. Luxburg, S. Bengio, H. Wallach, R. Fergus, S. Vish-

- wanathan, and R. Garnett, editors, *Proceedings of Neural Information Processing Systems (NeurIPS)*, 2017. 4, 5, 6
- [43] Ramakrishna Vedantam, C. Lawrence Zitnick, and Devi Parikh. CIDEr: Consensus-based image description evaluation. In *Proceedings of the IEEE/CVF Conference on Computer Vision and Pattern Recognition (CVPR)*, pages 4566–4575. IEEE Computer Society, 2015. 6
- [44] Erik Wijmans, Samyak Datta, Oleksandr Maksymets, Abhishek Das, Georgia Gkioxari, Stefan Lee, Irfan Essa, Devi Parikh, and Dhruv Batra. Embodied Question Answering in Photorealistic Environments with Point Cloud Perception. In *Proceedings of the IEEE/CVF Conference on Computer Vision and Pattern Recognition (CVPR)*, 2019. 1, 2, 3
- [45] Yi Wu, Yuxin Wu, Georgia Gkioxari, and Yuandong Tian. Building generalizable agents with a realistic and rich 3d environment. *arXiv preprint arXiv:1801.02209*, 2018. 2
- [46] Antoine Yang, Antoine Miech, Josef Sivic, Ivan Laptev, and Cordelia Schmid. Just ask: Learning to answer questions from millions of narrated videos. In *Proceedings of the IEEE/CVF International Conference on Computer Vision (ICCV)*, 2021. 3
- [47] Licheng Yu, Xinlei Chen, Georgia Gkioxari, Mohit Bansal, Tamara L. Berg, and Dhruv Batra. Multi-target embodied question answering. In *Proceedings of the IEEE/CVF Conference on Computer Vision and Pattern Recognition (CVPR)*, 2019. 1, 2
- [48] Licheng Yu, Patrick Poirson, Shan Yang, Alexander C. Berg, and Tamara L. Berg. Modeling context in referring expressions. In Bastian Leibe, Jiri Matas, Nicu Sebe, and Max Welling, editors, *Proceedings of the European Conference on Computer Vision (ECCV)*, pages 69–85, 2016. 1
- [49] Zhou Yu, Jun Yu, Yuhao Cui, Dacheng Tao, and Qi Tian. Deep modular co-attention networks for visual question answering. In *Proceedings of the IEEE/CVF Conference on Computer Vision and Pattern Recognition (CVPR)*, 2019. 2, 4, 5, 6, 1
- [50] Zhihao Yuan, Xu Yan, Yinghong Liao, Ruimao Zhang, Sheng Wang, Zhen Li, and Shuguang Cui. Instancerefer: Cooperative holistic understanding for visual grounding on point clouds through instance multi-level contextual referring. In *Proceedings of the IEEE/CVF International Conference on Computer Vision (ICCV)*, pages 1791–1800, 2021. 5
- [51] Lichen Zhao, Daigang Cai, Lu Sheng, and Dong Xu. 3dvg-transformer: Relation modeling for visual grounding on point clouds. In *Proceedings of the IEEE/CVF International Conference on Computer Vision (ICCV)*, pages 2928–2937, 2021. 5

Supplementary Material

In this supplementary material, we first show additional experimental details in Section A. Next, we provide additional experimental quantitative (Section B) and qualitative results (Section C). Finally, we attached a snapshot of the annotation website (Section D).

A. Additional Experimental Details

We conducted additional experiments to show the proposed method’s effectiveness compared to various methods. In this Section, we introduce other baselines and the additional ScanQA model that considers multiple objects related to a question.

A.1. Additional Baseline Models

Additional 2D-QA Image. We prepared RandomImage (or OracleImage) + 2D-QA as a 2D-QA baseline method that uses three images taken in the environment per question. Fig. 6 shows the images randomly sampled from the video to build the ScanNet dataset. In addition to using such real images from the environments, we also use images of ScanNet’s mesh data taken at positions and angles similar to real images as in Fig. 7. We refer to the models using real images “real” and ones using mesh images “mesh.” We also use mesh images taken from a top-down view (refer to Top-DownImage) to see the entire room with a single image, as in Fig. 8.

Additional 2D-QA Model. In addition to MCAN [49], we evaluated 2D-QA using a BERT-based model Oscar [28] trained with many image-text pairs, and has shown high performance in various tasks such as VQA, image retrieval, image captioning, and natural language visual reasoning. Although MCAN and Oscar use powerful pre-train models, unlike our method, we can emphasize the effectiveness of the ScanQA model by comparing it to these models.

A.2. Additional ScanQA Model

The ScanQA model introduced in Section 4 predicts object confidences (box confidences) and an object classification for a single object. However, a given question is sometimes associated with more than one object. Thus, we extended the ScanQA model to perform object localization and labeling for multiple objects. To this end, we computed final scores for all object proposals (or object labels) normalized by a sigmoid function and used BCE loss to train both object localization and object classification modules. The proposed method used in this paper is ScanQA (single), and the model that considers multiple objects is called ScanQA (multiple.) Hereafter, unless otherwise specified, ScanQA refers to ScanQA (single.)



Figure 6. Example of real images about a question “What color is the bathroom door?” Upper is RandomImage, lower is OracleImage.

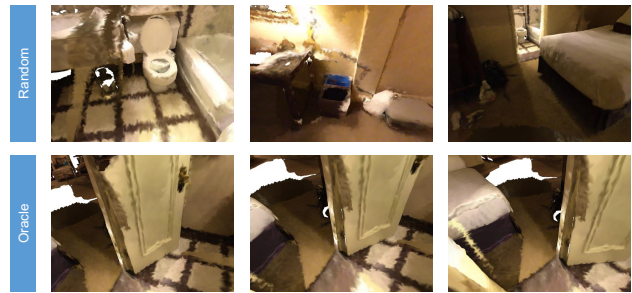


Figure 7. Example of mesh images about a question “What color is the bathroom door?” Upper is RandomImage, lower is OracleImage.

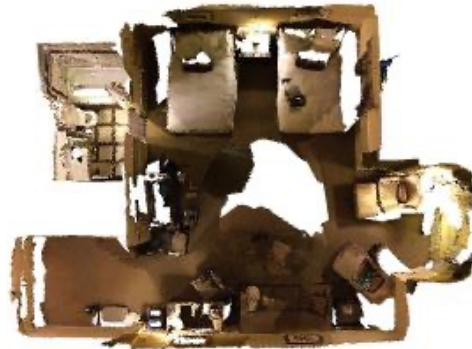


Figure 8. Example of a TopDownImage about a question “What color is the bathroom door?”

B. Additional Quantitative Experiments

B.1. Object Localization Results

Before introducing the additional QA results, we show object localization performance on ScanRefer+MCAN (pipeline), ScanRefer+MCAN (end-to-end), and ScanQA.

Model	Acc@0.25	Acc@0.5
Valid		
ScanRefer+MCAN (pipeline)	12.88	9.13
ScanRefer+MCAN (end-to-end)	23.53	11.76
ScanQA	24.96	15.42
Test w/ objects		
ScanRefer+MCAN (pipeline)	12.94	8.02
ScanRefer+MCAN (end-to-end)	21.97	10.41
ScanQA	25.44	15.03

Table 6. Object localization performance on the ScanQA dataset

We use the accuracy $\text{IoU}@K$ where the positive predictions have higher intersection over union (IoU) with the ground truths than the threshold K (set to 0.25 and 0.5) [10]. As in Table 5, we refer each accuracy to $\text{Acc}@0.25$ and $\text{Acc}@0.5$ in our experiments. The results in Table 6 show that shared and end-to-end learning of QA, object localization, and object classification modules effectively predicts the target object for a given question.

B.2. Question Answering Results

Table 8 shows the performance of additional baselines and proposed models on the ScanQA dataset. We show the best results in each column are shown in bold. The results show that our ScanQA (single or multiple) models outperformed other additional baselines RandomImage + MCAN (mesh), RandomImage + Oscar (mesh), TopDownImage + MCAN, and TopDownImage + Oscar across all evaluation metrics on all splits. While RandomImage + Oscar (real) outperformed ours on $\text{EM}@1$ on the test w/o objects split due to its powerful pre-trained model, ScanQA models outperformed RandomImage + Oscar (real) on other evaluation metrics. As for the difference using real and mesh images, the performance tends to be better when using real images. For example, RandomImage + MCAN (real) outperformed RandomImage + MCAN (mesh) and RandomImage + Oscar (real) outperformed RandomImage + Oscar (mesh) over almost evaluation measures on all splits. We observed no consistency of advantage regarding the performance difference between ScanQA (single) and ScanQA (multiple).

B.3. Ablation Studies on ScanQA (multiple)

In this Section, we conducted ablation studies on the ScanQA (multiple) model that predicts confidences and labels about multiple objects when performing QA. The effect of each major component of the proposed method is shown in Table 9, and the effect of different input data is shown in Table 7. The results in Table 9 suggest that using the object localization module (LOC) or the object classification module (OBJ) is effective for improving QA performance. Table 7 shows the object localization performance $\text{Top10-Acc}@0.25$ and QA performance $\text{EM}@10$

Model	Top10-Acc@0.25	EM@10
Valid		
ScanQA (xyz)	67.83	49.58
ScanQA (xyz+rgb)	66.72	50.22
ScanQA (xyz+rgb+normal)	68.13	49.45
ScanQA (xyz+multiview)	67.85	49.86
ScanQA (xyz+multiview+normal)	70.82	51.23
Test w/ objects		
ScanQA (xyz)	68.23	55.18
ScanQA (xyz+rgb)	68.87	56.23
ScanQA (xyz+rgb+normal)	69.65	55.25
ScanQA (xyz+multiview)	70.76	55.65
ScanQA (xyz+multiview+normal)	71.58	55.99

Table 7. Feature ablation results on ScanQA (multiple)

on ScanQA (multiple) using different input features, where $\text{Top10-Acc}@0.25$ is the accuracy where the positive predictions have higher IoU with the ground truth than 0.25 (we compare the top 10 object boxes with the highest object localization scores with the ground true boxes, and consider positive predictions for the box with the highest IoU.) We found RGB values are effective for QA and the multiview image features are effective for both object localization and QA. We assumed that by predicting multiple objects, ScanQA (multiple) was able to take advantage of those various features.

B.4. Performance by Parameter

We additionally show the performance of ScanQA with different parameters, the number of layers L and the hidden size d in Table 10 and in Table 11, respectively. The result suggests that the number of layers $L = 1$ and the hidden size $d = 128$ are suitable for the test splits.

B.5. Accuracy for Question Types

We classify the questions into six types: *object*, *color*, *object nature*, *place*, *number* and *other* by the beginning of the question sentences following Table 12. We evaluate the detailed question answering performance for each class for 2D-QA baselines and the ScanQA model. Table 13, Table 14 and Table 15 presents the detailed accuracy on valid, test w/ object and test w/o object respectively.

We notice that the performance scores for *place* questions is lower than other questions. We assume there are two reasons for this. First, there are several ways to answer the questions of *place*. Model predicts longer answers and therefor image captioning-based metrics are suitable rather than exact matching for *place* questions. For *color* questions, possible answers are limited and simple 2D-QA model can answer the questions from the sights of objects from several images. However, such answers are not grounded to objects in the questions.

Model	EM@1	EM@10	BLEU-1	BLEU-2	BLEU-3	BLEU-4	ROUGE	METEOR	CIDEr	SPICE
Valid										
RandomImage+MCAN (real)	19.19	48.15	23.71	15.41	11.81	0.00	28.90	10.92	53.83	9.35
RandomImage+MCAN (mesh)	18.59	47.81	22.12	14.49	11.72	7.69	27.61	10.32	50.93	8.37
RandomImage+Oscar (real)	19.38	46.37	22.91	14.52	11.20	0.56	28.70	10.66	52.86	8.91
RandomImage+Oscar (mesh)	17.97	43.55	20.67	12.01	11.51	0.57	26.51	9.82	47.82	7.75
TopDownImage+MCAN	12.71	41.50	14.82	8.21	16.54	0.74	19.33	7.57	33.14	5.72
TopDownImage+Oscar	17.20	43.81	19.75	11.21	15.31	0.71	25.39	9.43	45.21	7.32
VoteNet+MCAN	17.33	45.54	28.09	16.72	10.75	6.24	29.84	11.41	54.68	10.65
ScanRefer+MCAN (pipeline, real)	14.37	44.12	17.02	10.17	15.77	0.72	22.02	8.45	38.73	6.66
ScanRefer+MCAN (pipeline, mesh)	14.57	43.27	16.71	9.71	13.62	0.64	21.82	8.32	38.35	6.49
ScanRefer+MCAN (e2e)	18.59	46.76	26.93	16.59	11.59	7.87	30.03	11.52	55.41	11.28
ScanQA (single)	20.28	50.01	29.47	19.84	14.65	9.55	32.37	12.60	61.66	11.86
ScanQA (multiple)	21.05	51.23	30.24	20.40	15.11	10.08	33.33	13.14	64.86	13.43
OracleImage+MCAN (real)	22.59	49.43	26.58	18.32	15.37	8.50	33.23	12.45	63.44	12.56
OracleImage+MCAN (mesh)	20.66	48.04	24.35	17.00	14.23	0.00	30.34	11.23	57.01	10.15
OracleImage+Oscar (real)	21.39	45.05	24.29	14.19	14.21	0.67	31.24	11.33	58.23	10.51
OracleImage+Oscar (mesh)	22.27	46.59	23.01	13.96	14.23	0.00	31.37	11.53	57.98	11.11
Test w/ objects										
RandomImage+MCAN (real)	22.31	53.11	26.66	18.49	16.16	14.26	31.27	12.13	60.37	9.05
RandomImage+MCAN (mesh)	21.74	52.41	24.86	17.49	15.33	15.19	30.00	11.55	57.55	8.73
RandomImage+Oscar (real)	22.65	52.35	24.74	14.42	9.85	0.00	30.81	11.59	57.72	8.52
RandomImage+Oscar (mesh)	20.92	49.22	23.18	12.26	9.06	0.48	28.95	10.86	53.11	7.12
TopDownImage+MCAN	15.76	47.15	16.52	8.59	0.00	0.00	21.49	8.37	38.55	5.34
TopDownImage+Oscar	20.76	49.26	22.19	11.02	9.30	0.49	28.25	10.53	51.82	6.83
VoteNet+MCAN	19.71	50.76	29.46	17.23	10.33	6.08	30.97	12.07	58.23	10.44
ScanRefer+MCAN (pipeline, real)	17.52	49.92	19.17	10.66	0.00	0.00	24.40	9.38	44.25	6.24
ScanRefer+MCAN (pipeline, mesh)	17.44	48.83	18.45	9.49	0.00	0.00	23.90	9.11	42.97	5.93
ScanRefer+MCAN (e2e)	20.56	52.35	27.85	17.27	11.88	7.46	30.68	11.97	57.36	10.58
ScanQ (single)	23.45	56.51	31.56	21.39	15.87	12.04	34.34	13.55	67.29	11.99
ScanQA (multiple)	23.05	55.99	31.40	21.18	15.82	11.70	34.05	13.60	66.76	12.30
OracleImage+MCAN (real)	25.34	55.93	28.70	20.11	16.78	12.89	34.59	13.42	67.24	11.93
OracleImage+MCAN (mesh)	23.35	53.05	25.90	17.15	13.36	10.94	31.66	12.08	60.64	9.01
OracleImage+Oscar (real)	25.30	50.12	26.38	14.10	8.70	0.47	33.72	12.47	63.31	9.48
OracleImage+Oscar (mesh)	25.52	52.39	25.17	14.13	10.94	0.00	33.51	12.68	63.13	10.52
Test w/o objects										
RandomImage+MCAN (real)	20.82	51.23	26.29	17.90	14.27	9.66	29.23	11.54	55.64	8.87
RandomImage+MCAN (mesh)	20.34	51.20	24.72	16.93	14.04	7.55	28.10	10.95	53.41	8.61
RandomImage+Oscar (real)	21.58	49.85	24.86	16.16	13.29	0.00	28.99	10.99	54.62	8.62
RandomImage+Oscar (mesh)	19.91	48.74	23.02	13.24	12.91	0.64	26.94	10.17	49.83	7.45
TopDownImage+MCAN	14.39	45.94	15.70	8.86	12.56	0.62	19.26	7.71	34.59	5.22
TopDownImage+Oscar	19.13	48.06	21.93	11.66	14.64	0.70	25.98	9.67	47.37	6.93
VoteNet+MCAN	18.15	48.56	29.63	17.80	11.57	7.10	29.12	11.68	53.34	10.36
ScanRefer+MCAN (pipeline, real)	16.47	49.05	18.71	10.97	16.53	0.76	22.45	8.76	40.81	6.41
ScanRefer+MCAN (pipeline, mesh)	16.39	47.76	18.28	10.42	15.03	0.71	22.07	8.62	40.19	6.03
ScanRefer+MCAN (e2e)	19.04	49.70	26.98	16.17	11.28	7.82	28.61	11.38	53.41	10.63
ScanQA (single)	20.90	54.11	30.68	21.20	15.81	10.75	31.09	12.59	60.24	11.29
ScanQA (multiple)	21.30	53.05	31.14	21.20	15.81	11.18	31.62	12.82	60.95	11.68

Table 8. Performance comparison for question answering with image captioning metrics.

C. Additional Qualitative Analysis

We conducted a qualitative evaluation by comparing our ScanQA model to the ScanRefer + MCAN (end-to-end) in addition to the evaluation on ScanRefer + MCAN (pipeline) as in Fig. 5. The results in Fig. 9 show the object localization and QA correctness with the visualization of the scene and bounding boxes by the ScanRefer + MCAN (end-to-end), ScanQA, and ground truth (GT). The results also show that QA correctness and localization are closely related. The leftmost case shows that models should answer the color of the bathrobe. However, the baseline model, ScanRefer + MCAN (end-to-end), localized a different object “table” and answered its color. The baseline model used the word “wall” to find an object near the wall and

localized it. On the other hand, our model could localize the correct object, “bathrobe,” on the wall. In the second from the left case, the question is about the object placed on the chair, but the baseline model gives the wrong answer “table” because the word “seat” is usually associated with the table. In contrast, our model understands the meaning “in the seat” and correctly selects a backpack in the seat. In the second case from the right, the baseline model incorrectly localized a TV close to the wall and answered “chair” close to the TV. Our model correctly recognized the meaning “corner,” localized it, and answered the correct object “trash can” at the corner. In the last case, there are multiple ottomans in the scene, and the models need to correctly understand the positional relationship between the ottoman,

ANS	OBJ	LOC	EM@1	EM@10	BLEU-1	BLEU-2	BLEU-3	BLEU-4	ROUGE	METEOR	CIDEr	SPICE
Valid												
✓			7.53	27.70	8.30	6.03	0.15	0.02	10.14	4.47	21.04	2.21
✓	✓		19.87	49.43	29.26	18.75	13.03	7.30	31.98	12.28	60.63	11.98
✓		✓	20.47	50.05	28.34	19.03	14.16	9.95	31.91	12.25	61.02	11.69
✓	✓	✓	21.05	51.23	30.24	20.40	15.11	10.08	33.33	13.14	64.86	13.43
Test w/ objects												
✓			8.20	32.68	8.10	5.57	0.14	0.02	10.09	4.29	21.02	1.89
✓	✓		22.07	55.10	30.44	19.85	14.33	10.18	32.89	13.06	63.93	11.51
✓		✓	23.77	55.31	30.65	21.42	16.61	13.37	34.15	13.40	66.69	10.88
✓	✓	✓	23.05	55.99	31.40	21.18	15.82	11.70	34.05	13.60	66.76	12.30
Test w/o objects												
✓			8.41	31.42	8.40	5.48	0.14	0.02	10.32	4.35	20.64	1.68
✓	✓		20.80	53.70	31.30	20.51	14.58	10.48	31.51	12.75	60.09	11.75
✓		✓	20.90	53.78	30.01	22.39	17.98	13.79	30.69	12.51	60.37	11.34
✓	✓	✓	21.30	53.05	31.14	21.20	15.81	11.18	31.62	12.82	60.95	11.68

Table 9. Performance comparison between the different experimental conditions of the ScanQA (multiple) model.

Model	EM@1	EM@10	BLEU-1	BLEU-2	BLEU-3	BLEU-4	ROUGE	METEOR	CIDEr	SPICE
Valid										
ScanQA ($L = 1$)	19.96	49.78	29.49	19.16	13.23	8.44	32.35	12.59	61.14	12.61
ScanQA ($L = 2$)	20.28	50.01	29.47	19.84	14.65	9.55	32.37	12.60	61.66	11.86
ScanQA ($L = 3$)	11.94	39.14	13.93	8.82	7.23	0.00	18.64	6.98	33.30	6.55
Test w/ objects										
ScanQA ($L = 1$)	23.83	55.63	32.64	21.80	15.63	11.67	35.20	14.15	69.70	12.65
ScanQA ($L = 2$)	23.45	56.51	31.56	21.39	15.87	12.04	34.34	13.55	67.29	11.99
ScanQA ($L = 3$)	13.83	44.71	15.05	7.90	5.84	0.00	19.62	7.34	36.38	5.62
Test w/o objects										
ScanQA ($L = 1$)	21.01	52.50	31.23	21.37	15.97	11.20	31.55	12.84	61.11	11.82
ScanQA ($L = 2$)	20.90	54.11	30.68	21.20	15.81	10.75	31.09	12.59	60.24	11.29
ScanQA ($L = 3$)	11.63	40.30	13.42	7.75	5.96	0.00	16.75	6.43	29.86	5.13

Table 10. Performance comparison for the ScanQA model with difference number of layers L

chair, and pillow. The baseline model localized the lamp and incorrectly answered its color “white.” In contrast, our model correctly understands the positional relationship between the ottoman, chair, and pillow localizing the ottoman in front of the chair with a pillow.

D. MTurk Annotation Details

We developed a visualizer website for 3D modelings. MTurk workers can interactively rotate and zoom in the 3D modeling. Fig. 10 presents the snapshot of the MTurk website for the editing and answer collection phrase of the QA annotation.

Model	EM@1	EM@10	BLEU-1	BLEU-2	BLEU-3	BLEU-4	ROUGE	METEOR	CIDEr	SPICE
Valid										
ScanQA ($d = 128$)	20.88	50.70	30.08	20.62	15.72	11.18	33.25	12.97	64.09	12.77
ScanQA ($d = 256$)	20.28	50.01	29.47	19.84	14.65	9.55	32.37	12.60	61.66	11.86
ScanQA ($d = 512$)	13.99	41.54	17.01	11.02	8.26	0.00	21.97	8.11	38.78	6.89
Test w/ objects										
ScanQA ($d = 128$)	24.38	56.71	32.30	22.47	17.98	14.96	35.24	14.07	69.53	12.61
ScanQA ($d = 256$)	23.45	56.51	31.56	21.39	15.87	12.04	34.34	13.55	67.29	11.99
ScanQA ($d = 512$)	14.75	46.02	16.89	9.18	7.06	6.77	21.17	7.76	38.56	5.47
Test w/o objects										
ScanQA ($d = 128$)	21.17	54.20	31.79	22.23	16.65	11.32	31.83	13.01	61.92	12.13
ScanQA ($d = 256$)	20.90	54.11	30.68	21.20	15.81	10.75	31.09	12.59	60.24	11.29
ScanQA ($d = 512$)	12.83	43.28	16.67	9.56	7.01	4.70	18.97	7.31	33.63	5.08

Table 11. Performance comparison for the ScanQA model with difference hidden size d

Question type	Question beginning	# Instances in the valid set
Object	<i>What is</i> (except questions classified as color)	1476
Color	<i>What color</i> <i>What is the color</i>	838
Object nature	<i>What type</i> <i>What shape</i> <i>What kind</i>	358
Place	<i>Where is</i>	963
Number	<i>How many</i>	224
Other	(remaining questions)	814

Table 12. Question type and the beginning of the question sentence.

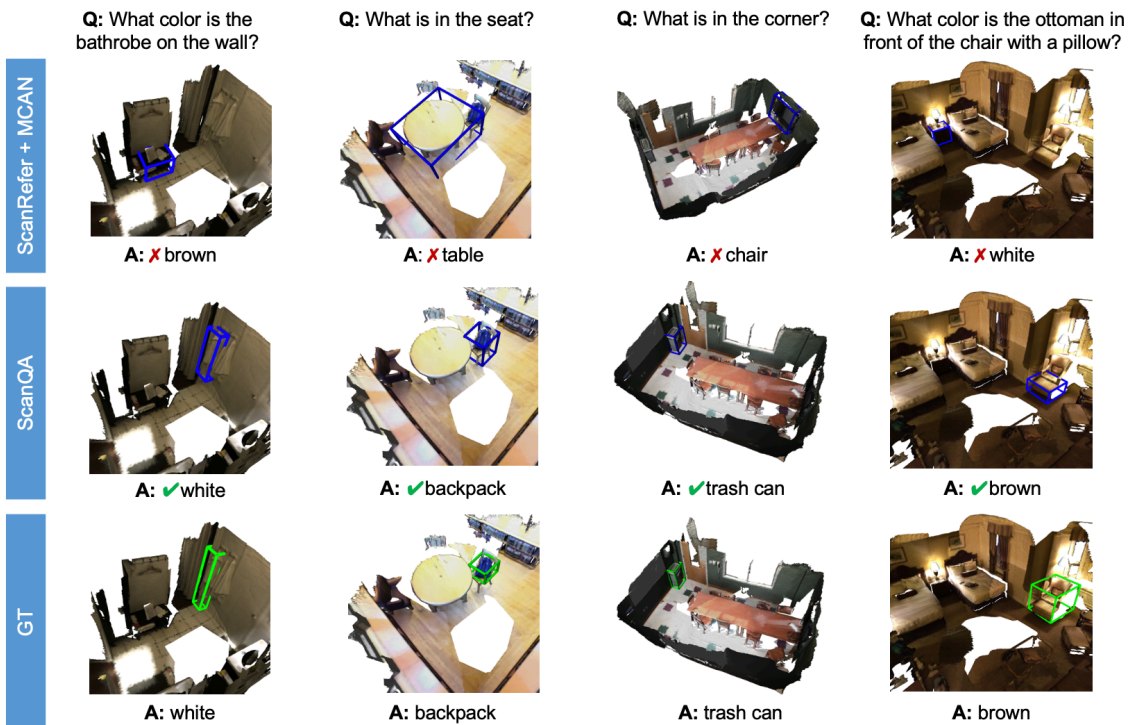


Figure 9. Qualitative analysis comparing ScanQA and ScanRefer + MCAN (end-to-end).

Model	EM@1	EM@10	BLEU-1	BLEU-2	BLEU-3	BLEU-4	ROUGE	METEOR	CIDEr	SPICE
Object										
RandomImage+MCAN	15.02	45.06	20.33	16.22	17.13	0.79	43.03	9.18	22.18	14.03
VoteNet+MCAN	12.31	41.07	20.81	13.51	6.47	0.00	39.81	8.88	21.37	14.09
ScanRefer+MCAN (pipeline)	11.84	38.09	15.91	12.73	0.23	0.03	32.64	7.37	17.49	12.40
ScanRefer+MCAN (e2e)	14.82	42.76	20.43	15.57	8.19	0.00	41.74	9.00	22.12	14.87
ScanQA (single)	17.52	45.47	23.94	18.19	0.00	0.00	50.05	10.62	26.01	17.57
ScanQA (multiple)	18.27	47.70	26.15	19.19	14.46	0.00	53.84	11.53	27.52	18.46
Color										
RandomImage+MCAN	44.03	86.04	45.92	31.38	0.44	0.05	86.65	23.57	49.36	2.19
VoteNet+MCAN	41.65	81.62	47.01	28.19	20.58	0.01	86.54	23.32	49.01	3.09
ScanRefer+MCAN (pipeline)	30.79	83.41	32.75	0.05	0.01	0.00	59.01	16.14	34.87	0.00
ScanRefer+MCAN (e2e)	44.99	83.77	46.72	35.91	0.00	0.00	87.75	24.16	50.13	1.85
ScanQA (single)	42.60	83.53	43.92	29.48	0.00	0.00	84.42	22.61	47.68	1.39
ScanQA (multiple)	42.60	85.44	45.23	17.78	0.00	0.00	85.20	22.76	48.34	2.41
Object nature										
RandomImage+MCAN	18.16	47.49	31.06	26.40	26.83	1.07	57.15	13.18	33.69	7.11
VoteNet+MCAN	17.04	47.77	35.70	23.15	16.71	0.00	62.83	14.66	35.21	16.42
ScanRefer+MCAN (pipeline)	15.36	43.30	20.14	16.72	18.38	0.77	38.60	9.25	27.09	2.27
ScanRefer+MCAN (e2e)	13.41	48.32	36.50	20.03	16.41	0.00	58.03	14.50	34.75	16.08
ScanQA (single)	18.44	51.40	41.65	25.65	18.81	0.00	73.26	16.54	41.61	17.16
ScanQA (multiple)	20.11	54.75	41.34	29.72	25.80	0.01	78.31	17.31	40.54	18.67
Place										
RandomImage+MCAN	3.95	17.24	17.87	11.59	8.29	0.00	33.58	8.05	19.00	11.55
VoteNet+MCAN	4.88	18.48	28.31	17.84	12.07	7.47	45.08	9.97	26.41	14.68
ScanRefer+MCAN (pipeline)	2.08	11.53	8.26	5.08	0.11	0.02	14.34	5.29	9.65	5.74
ScanRefer+MCAN (e2e)	4.98	17.86	25.31	15.64	11.20	8.01	44.72	9.87	25.06	15.98
ScanQA (single)	6.85	23.16	28.78	19.48	14.41	9.55	57.00	11.49	28.19	16.66
ScanQA (multiple)	7.79	23.99	28.21	19.13	14.27	9.92	59.34	11.46	28.30	18.13
Number										
RandomImage+MCAN	39.29	86.16	45.01	0.06	0.01	0.00	72.26	19.55	46.70	0.00
VoteNet+MCAN	36.16	86.16	43.77	20.59	0.33	0.04	67.56	18.13	44.02	0.40
ScanRefer+MCAN (pipeline)	38.39	85.71	44.26	0.06	0.01	0.00	67.76	19.37	45.69	0.00
ScanRefer+MCAN (e2e)	34.82	84.82	39.01	0.06	0.01	0.00	61.06	17.01	40.78	0.00
ScanQA (single)	39.29	85.71	44.29	0.00	0.00	0.00	72.15	19.16	46.05	0.00
ScanQA (multiple)	40.62	85.71	46.00	44.09	0.55	0.06	75.68	19.80	47.72	0.45
Other										
RandomImage+MCAN	14.13	41.15	18.93	13.19	11.63	0.54	42.28	8.83	24.75	9.17
VoteNet+MCAN	11.06	36.36	20.87	7.91	0.00	0.00	36.71	8.61	23.29	7.68
ScanRefer+MCAN (pipeline)	10.69	37.22	17.28	10.45	0.18	0.02	33.89	8.12	21.74	6.98
ScanRefer+MCAN (e2e)	12.16	38.94	21.10	12.82	8.29	0.00	42.69	9.32	24.54	9.91
ScanQA (single)	14.13	43.37	22.26	13.72	8.02	0.00	45.39	9.96	26.30	10.78
ScanQA (multiple)	14.62	43.61	23.52	15.64	9.61	0.00	47.89	10.39	27.26	11.34

Table 13. Valid set performance comparison for question answering with image captioning metrics. **e2e** represents an end-to-end model.

Model	EM@1	EM@10	BLEU-1	BLEU-2	BLEU-3	BLEU-4	ROUGE	METEOR	CIDEr	SPICE
Object										
RandomImage+MCAN	16.47	46.59	22.68	18.15	0.00	0.00	47.16	9.69	23.49	15.65
VoteNet+MCAN	13.23	43.84	21.32	13.72	7.47	5.36	40.98	8.80	21.05	14.25
ScanRefer+MCAN (pipeline)	12.74	41.24	15.87	12.36	0.23	0.03	33.82	7.10	17.32	13.24
ScanRefer+MCAN (e2e)	15.97	46.24	21.12	15.76	6.96	0.00	43.01	9.13	22.28	15.87
ScanQA (single)	18.86	49.96	24.75	18.78	13.73	10.62	51.81	10.68	26.00	17.09
ScanQA (multiple)	19.14	52.15	26.78	20.97	17.86	17.64	55.24	11.25	26.98	18.47
Color										
RandomImage+MCAN	45.56	89.56	49.39	50.81	0.62	0.07	91.84	25.87	50.08	2.08
VoteNet+MCAN	40.57	84.66	48.05	23.43	11.85	0.00	85.40	23.56	47.41	2.28
ScanRefer+MCAN (pipeline)	31.24	86.69	36.03	0.06	0.01	0.00	62.00	17.61	35.67	0.00
ScanRefer+MCAN (e2e)	41.96	88.08	47.76	27.33	0.00	0.00	84.52	24.04	47.74	2.22
ScanQA (single)	45.75	88.45	50.27	22.71	0.00	0.00	92.54	26.06	50.96	2.10
ScanQA (multiple)	43.25	88.54	48.71	12.31	0.00	0.00	88.00	24.53	48.83	2.14
Object nature										
RandomImage+MCAN	19.91	50.98	35.93	25.12	23.14	0.98	56.79	13.73	35.93	6.54
VoteNet+MCAN	19.91	49.45	38.95	22.65	0.00	0.00	61.17	14.90	36.42	18.18
ScanRefer+MCAN (pipeline)	19.69	46.17	27.85	23.18	0.00	0.00	47.31	11.42	33.08	2.33
ScanRefer+MCAN (e2e)	19.04	50.33	39.23	23.34	17.01	0.00	61.06	14.71	35.99	15.24
ScanQA (single)	22.98	56.67	45.09	28.98	21.27	0.96	72.81	16.85	41.52	14.79
ScanQA (multiple)	22.76	55.14	45.76	29.72	18.14	0.00	72.16	17.15	41.77	16.95
Place										
RandomImage+MCAN	3.97	16.10	19.50	14.32	13.07	11.67	39.74	8.68	19.87	10.97
VoteNet+MCAN	4.43	17.62	28.82	18.10	11.84	7.05	46.59	10.31	26.70	15.02
ScanRefer+MCAN (pipeline)	1.40	9.68	7.33	3.65	0.09	0.01	11.45	5.11	8.52	4.45
ScanRefer+MCAN (e2e)	4.08	18.20	24.31	15.62	11.18	7.35	43.72	9.64	24.54	14.32
ScanQA (single)	7.12	22.17	29.59	20.93	16.47	12.59	61.89	12.06	29.35	18.17
ScanQA (multiple)	5.95	21.94	26.89	18.87	14.53	10.60	55.13	11.11	27.10	16.74
Number										
RandomImage+MCAN	43.14	90.20	44.97	0.06	0.01	0.00	83.02	23.81	46.94	0.00
VoteNet+MCAN	39.61	90.98	44.01	16.07	0.29	0.04	75.94	21.71	44.29	0.72
ScanRefer+MCAN (pipeline)	43.53	89.41	45.32	0.06	0.01	0.00	81.52	23.89	47.48	0.00
ScanRefer+MCAN (e2e)	34.12	87.84	36.29	0.00	0.00	0.00	63.70	18.28	37.43	0.00
ScanQA (single)	40.78	90.59	44.94	0.00	0.00	0.00	77.33	22.44	45.80	0.00
ScanQA (multiple)	37.25	90.59	40.25	22.86	0.36	0.05	72.15	20.07	41.37	0.39
Other										
RandomImage+MCAN	16.37	45.46	19.02	12.93	0.00	0.00	42.83	9.01	24.99	9.02
VoteNet+MCAN	13.72	41.81	20.85	9.92	3.53	0.00	41.08	8.81	24.41	8.72
ScanRefer+MCAN (pipeline)	15.04	42.48	18.00	10.61	0.19	0.03	37.78	8.51	23.46	6.42
ScanRefer+MCAN (e2e)	14.71	42.59	21.09	11.01	7.21	0.00	41.46	9.23	24.70	9.36
ScanQA (single)	17.92	46.79	24.50	15.76	9.92	7.06	50.88	10.66	28.78	11.69
ScanQA (multiple)	17.37	46.02	23.94	14.30	8.00	0.00	50.63	10.55	28.06	11.58

Table 14. Test w/ object set performance comparison for question answering with image captioning metrics. **e2e** represents an end-to-end model.

Model	EM@1	EM@10	BLEU-1	BLEU-2	BLEU-3	BLEU-4	ROUGE	METEOR	CIDEr	SPICE
Object										
RandomImage+MCAN	15.85	44.84	22.37	17.97	15.07	0.73	41.56	9.29	22.39	14.41
VoteNet+MCAN	13.80	42.52	20.65	12.39	5.86	0.00	37.06	8.71	20.69	14.79
ScanRefer+MCAN (pipeline)	12.48	41.14	17.70	14.87	0.27	0.04	32.31	7.44	17.52	12.95
ScanRefer+MCAN (e2e)	14.30	44.56	20.26	15.31	9.77	0.00	37.90	8.67	20.56	15.61
ScanQA (single)	17.39	49.75	24.79	18.87	11.47	0.00	46.97	10.36	24.89	16.73
ScanQA (multiple)	18.83	48.48	25.96	21.26	16.90	0.00	49.72	11.00	25.95	17.00
Color										
RandomImage+MCAN	43.31	89.38	45.74	0.00	0.00	0.00	87.49	24.55	46.66	0.90
VoteNet+MCAN	38.62	83.00	44.74	15.35	11.79	0.63	79.21	22.16	44.35	1.03
ScanRefer+MCAN (pipeline)	33.46	87.77	36.88	0.06	0.01	0.00	67.21	18.88	36.90	0.00
ScanRefer+MCAN (e2e)	40.15	85.23	44.53	0.00	0.00	0.00	81.64	22.92	44.72	0.71
ScanQA (single)	40.00	87.85	43.58	0.00	0.00	0.00	80.77	22.60	43.89	0.54
ScanQA (multiple)	40.92	87.46	44.15	14.64	0.00	0.00	82.22	22.96	44.62	0.77
Object nature										
RandomImage+MCAN	15.17	41.67	29.06	25.84	23.07	0.98	47.21	11.46	27.54	7.27
VoteNet+MCAN	10.68	41.45	33.29	18.02	11.91	0.00	45.85	12.37	28.44	15.82
ScanRefer+MCAN (pipeline)	13.46	39.74	20.73	22.67	25.65	1.03	35.67	8.29	22.18	3.46
ScanRefer+MCAN (e2e)	13.25	39.32	34.51	19.23	13.25	0.00	51.52	12.96	30.13	18.28
ScanQA (single)	15.60	46.15	41.96	28.75	19.96	0.92	65.48	15.62	35.60	20.89
ScanQA (multiple)	13.68	47.65	41.40	25.58	20.39	0.01	59.70	14.75	34.43	19.06
Place										
RandomImage+MCAN	4.76	19.34	21.88	14.48	11.08	7.76	41.12	9.18	22.08	12.85
VoteNet+MCAN	5.85	20.20	32.15	20.62	13.86	8.80	50.54	11.16	29.06	16.43
ScanRefer+MCAN (pipeline)	1.64	11.93	8.87	4.58	0.11	0.02	12.82	5.34	9.14	5.42
ScanRefer+MCAN (e2e)	4.99	21.14	24.47	15.03	10.76	7.95	44.46	9.57	23.99	15.05
ScanQA (single)	6.79	26.37	32.47	23.04	18.34	13.74	63.40	12.27	29.67	19.28
ScanQA (multiple)	6.79	24.57	30.18	20.39	15.19	10.81	56.65	11.37	27.97	17.71
Number										
RandomImage+MCAN	42.51	90.64	45.13	0.07	0.01	0.00	77.60	22.40	45.21	0.00
VoteNet+MCAN	33.69	90.64	40.35	25.05	0.40	0.05	63.81	18.53	38.63	0.27
ScanRefer+MCAN (pipeline)	41.44	90.64	44.12	0.06	0.01	0.00	74.31	22.01	44.17	0.00
ScanRefer+MCAN (e2e)	37.97	89.30	41.12	0.00	0.00	0.00	70.08	19.69	40.83	0.00
ScanQA (single)	36.90	90.64	42.69	28.69	0.43	0.05	68.30	19.57	41.43	0.00
ScanQA (multiple)	40.91	90.64	46.20	29.85	0.44	0.05	77.26	21.84	45.16	0.00
Other										
RandomImage+MCAN	15.21	43.11	18.74	14.85	15.93	0.72	40.50	8.65	22.32	8.13
VoteNet+MCAN	12.36	37.75	20.15	9.26	3.22	0.00	33.82	8.25	20.73	7.64
ScanRefer+MCAN (pipeline)	11.82	40.81	16.74	11.26	0.00	0.00	32.49	7.23	19.04	5.50
ScanRefer+MCAN (e2e)	13.35	38.51	20.31	9.82	6.21	0.00	37.70	8.73	22.34	9.12
ScanQA (single)	15.32	41.79	21.99	12.74	6.92	0.00	40.30	9.30	23.99	10.33
ScanQA (multiple)	14.55	40.48	20.69	12.93	8.57	6.81	38.74	8.69	22.53	9.22

Table 15. Test w/o object set performance comparison for question answering with image captioning metrics. **e2e** represents an end-to-end model.

Left-drag to rotate, right-drag to move. Scroll to zoom in/out. Use the show object IDs checkbox. It may take some time to show the 3D modeling.



Questions	Check when the original question is valid and answerable	Rewrite (refine) the question	Object IDs	Answer phrase / words
What color is the door at the entrance to the room?	<input type="checkbox"/> This question is answerable	<input type="text"/>	<input type="text"/>	<input type="text"/>

Figure 10. Example of 3D modeling viewer and QA form on the MTurk website.